

# Do We Understand What the Mercury Speciation Instruments Are Actually Measuring? Results of RAMIX

Part of the "RAMIX: Reno Atmospheric Intercomparison eXperiment" group

Mae Sexauer Gustin,<sup>†,\*</sup> Jiaoyan Huang,<sup>†</sup> Matthieu B. Miller,<sup>†</sup> Christianna Peterson,<sup>†</sup> Daniel A. Jaffe,<sup>‡,§</sup> Jesse Ambrose,<sup>‡</sup> Brandon D. Finley,<sup>‡</sup> Seth N. Lyman,<sup>‡,◆</sup> Kevin Call,<sup>‡</sup> Robert Talbot,<sup>||</sup> Dara Feddersen,<sup>⊥</sup> Huiting Mao,<sup>#</sup> and Steven E. Lindberg<sup>▽</sup>

<sup>†</sup>Department of Natural Resources and Environmental Science, University of Nevada, Reno, 1664 N. Virginia Street, Reno, Nevada, United States, 89557

<sup>‡</sup>Science and Technology Program, University of Washington—Bothell, 18115 Campus Way NE, Bothell, Washington, United States, 98011

<sup>§</sup>Department of Atmospheric Sciences, University of Washington, Seattle, Washington, United States, 98195

<sup>||</sup>Department of Earth and Atmospheric Science, University of Houston, Houston, Texas, United States, 77204

<sup>⊥</sup>Department of Chemistry, University of New Hampshire, Durham, New Hampshire, United States, 03824

<sup>#</sup>Department of Chemistry, State University of New York, College of Environmental Science and Forestry, Syracuse, New York, United States, 13210

<sup>▽</sup>Emeritus Fellow, Oak Ridge National Laboratory, Graeagle, California

## Supporting Information

**ABSTRACT:** From August 22 to September 16, 2012, atmospheric mercury (Hg) was measured from a common manifold in the field during the Reno Atmospheric Mercury Intercomparison eXperiment. Data were collected using Tekran systems, laser induced fluorescence, and evolving new methods. The latter included the University of Washington-Detector for Oxidized Mercury, the University of Houston Mercury instrument, and a filter-based system under development by the University of Nevada-Reno. Good transmission of total Hg was found for the manifold. However, despite application of standard protocols and rigorous quality control, systematic differences in operationally defined forms of Hg were measured by the sampling systems. Concentrations of reactive Hg (RM) measured with new methods were at times 2-to-3-fold higher than that measured by Tekran system. The low RM recovery by the latter can be attributed to lack of collection as the system is currently configured. Concentrations measured by all instruments were influenced by their sampling location in-the-manifold and the instrument analytical configuration. On the basis of collective assessment of the data, we hypothesize that reactions forming RM were occurring in the manifold. Results provide a new framework for improved understanding of the atmospheric chemistry of Hg.



## INTRODUCTION

Atmospheric mercury (Hg) is currently measured as gaseous elemental Hg (GEM, generally 1 to 3 ng m<sup>-3</sup>), gaseous oxidized (GOM), and particle bound (PBM).<sup>1,2</sup> Gaseous elemental Hg is thought to constitute 90 to 99% of the Hg in the atmosphere and to be relatively inert. The chemical forms of GOM have not been identified and the mechanisms important for formation are uncertain. Suggested compounds include HgCl<sub>2</sub>, HgBr<sub>2</sub>, HgO, HgSO<sub>4</sub>, Hg(NO<sub>2</sub>)<sub>2</sub>, and Hg(OH)<sub>2</sub>.<sup>3–12</sup> In general, our understanding of PBM is poor; however, temperature is considered to play an important role in partitioning between the gas and particle phase.<sup>13</sup>

The automated method widely used to measure atmospheric Hg is the Tekran 2537/1130/1135 system (Tekran Instrument Corp., Ontario, Canada). This system applies a specific set of collection and desorption procedures resulting in operationally defined quantification of GEM, GOM, and PBM, respectively (see Supporting Information, SI). A KCl-coated quartz annular denuder is used to collect GOM; PBM is collected on a column

**Received:** September 26, 2012

**Revised:** December 31, 2012

**Accepted:** January 10, 2013



of quartz chips and a quartz filter; and GEM is concentrated on patented dual gold cartridges, in this order. Once collected, Hg is thermally desorbed from each unit and quantified as GEM using Cold Vapor Atomic Fluorescence Spectroscopy (CVAFS).<sup>14,15</sup> There are no standard reference materials for GOM or PBM, and interferences for this instrument have not been adequately explored.<sup>16,17</sup> Reported precision between colocated instruments is 0.4 to 20%, 15 to 40%, and up to 70% for GEM, GOM, and PBM, respectively.<sup>18–23</sup> The 2537 unit alone is often used to measure atmospheric Hg independent of the 1130 and 1135 units. There is debate as to whether data collected using the 2537 unit are total atmospheric Hg (TM = GEM + GOM + PBM), GEM, or some fraction of all forms.<sup>16,24–26</sup>

Over time, multiple researchers have tested components of this system and compared observations with those obtained using other methods (see discussion and references in the SI). Concerns raised include passivation of the gold surface used to collect GEM, the impact of ozone ( $O_3$ ) and water vapor on the collection of GOM by the denuder and particle collecting units, the ability of the denuder to collect all forms of GOM, and artifacts associated with the PBM measurement. Without accurate, precise measurements of atmospheric Hg, we cannot understand the chemistry, interpret observed spatial and temporal patterns, or improve models.

Here, we present the results of a comparison of data collected using two Tekran 2537/1130/1135 systems, two Tekran 2537 units, the Detector for Oxidized Hg Species (DOHGS) designed by University of Washington-Bothell (UW), and the University of Houston Mercury instrument (UHMERC) system operated by a team from the University of Houston, the State University of New York, and the University of New Hampshire. These instruments measured air Hg concentrations from a common manifold<sup>27</sup> in the field during the Reno Atmospheric Mercury Intercomparison eXperiment (RAMIX). Additional free-standing (adjacent but not connected to the manifold) measurements were made using the Tekran systems during and after RAMIX. Limited measurements were also made using a nylon filter system designed by the University of Nevada-Reno (UNR).<sup>28</sup> Desert Research Institute operated a cavity ring-down spectroscopy system;<sup>29</sup> however, because of strong drifts in baseline extinction due to laser problems, they did not obtain any data that could be used for the comparisons presented in this work. Here, we present free-standing and in-the-manifold data collected using the Tekran system, and compare with new methods. These are applied collectively to investigate the atmospheric chemistry of Hg during RAMIX.

**Field Setting.** The RAMIX project was held at an inactive Hg Deposition Network (MDN, <http://nadp.sws.uiuc.edu/mdn>) site, MDN NV98, located on the UNR Agricultural Experiment Station property (39.51° latitude, -119.72° longitude, elevation 1340 m) (ref 30 and SI). The designated RAMIX sampling time period occurred over four weeks from August 22 to September 16, 2012.

**Air Sampling Methods.** All units sampled from a common manifold system consisting of 2.54 cm outer diameter (O.D.) insulated Teflon PFA tubing (see SI<sup>27</sup>) situated between four trailers housing equipment (only two shown in Figure 1). The upstream end of the manifold was a Teflon-coated cyclone inlet (URG-2000-30EA) with a cut size of 1  $\mu\text{m}$  (50%) at a flow rate of 200  $\text{L min}^{-1}$  (manufacturer communication). Mean flow in-the-manifold was  $210 \pm 4 \text{ L min}^{-1}$ , and ranged from 187 to

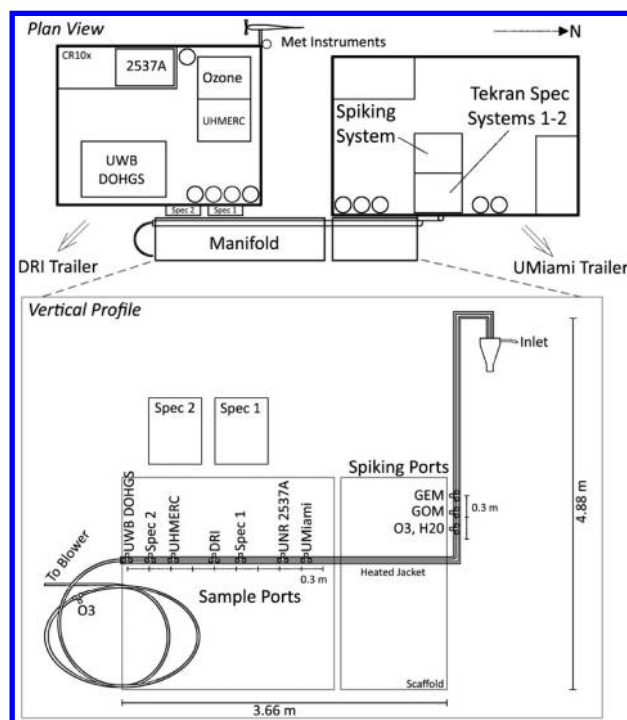


**Figure 1.** Schematic map of the trailers housing the equipment described in this paper (top panel) and a vertical profile of the manifold system (bottom panel). Note two other trailers were also present at the site. The CO instrument was located below the Spiking System in the large trailer. Circles indicate gas cylinders.

238  $\text{L min}^{-1}$ . The first 6 m of the manifold, including the cyclone inlet and the active sampling area, were insulated and heated to  $115 \pm 2 \text{ }^{\circ}\text{C}$  (Figure 1; see SI and ref 27 for details).

Prior to RAMIX, testing of a manifold system of similar configuration, but  $\sim 75\%$  shorter length, was done at UW using laboratory air. Finley et al.<sup>27</sup> described the estimated transmission efficiency as 83 to 102% for GEM,  $96 \pm 3\%$  for  $O_3$ , and  $78 \pm 4\%$  (range 73 to 88%) for  $\text{HgBr}_2$ . During this laboratory study and RAMIX, GEM spikes were observed within 5 min based on the Tekran analytical cycle. Laboratory tests at UW prior to RAMIX indicated that 10 min were needed for  $\text{HgBr}_2$  concentrations to become stable, and to be removed from the system.<sup>27</sup> To account for this in the data analyses, the first 5 min of GEM spikes were not included when assessing recoveries and instrument responses, and  $\text{HgBr}_2$  spikes were started 1 h before sampling.

Gaseous elemental Hg was added to the manifold during Weeks 1 to 4 of the experiment.  $\text{HgBr}_2$ ,  $O_3$ , and  $\text{H}_2\text{O}$  vapor were added in Weeks 3 and 4. During Week 4, data were collected simultaneously using a free-standing Tekran system, and one sampling from the manifold. Limited simultaneous spikes were done, and conclusions regarding these are not possible; however, to help future researchers the details are provided in the SI. On the basis of temperature sensitivity of the flow sensor at the end of the manifold, spike recovery values have an uncertainty of  $\pm 15\%$ .

During RAMIX, UNR operated two Tekran 2537/1130/1135 atmospheric Hg speciation systems, hereafter referred to as Spec 1, the first in the line moving down flow, and Spec 2, the second in-line. In addition, to these Tekran systems UNR operated a Tekran 2537 unit, two  $O_3$  analyzers, a carbon monoxide (CO) analyzer, and meteorological equipment

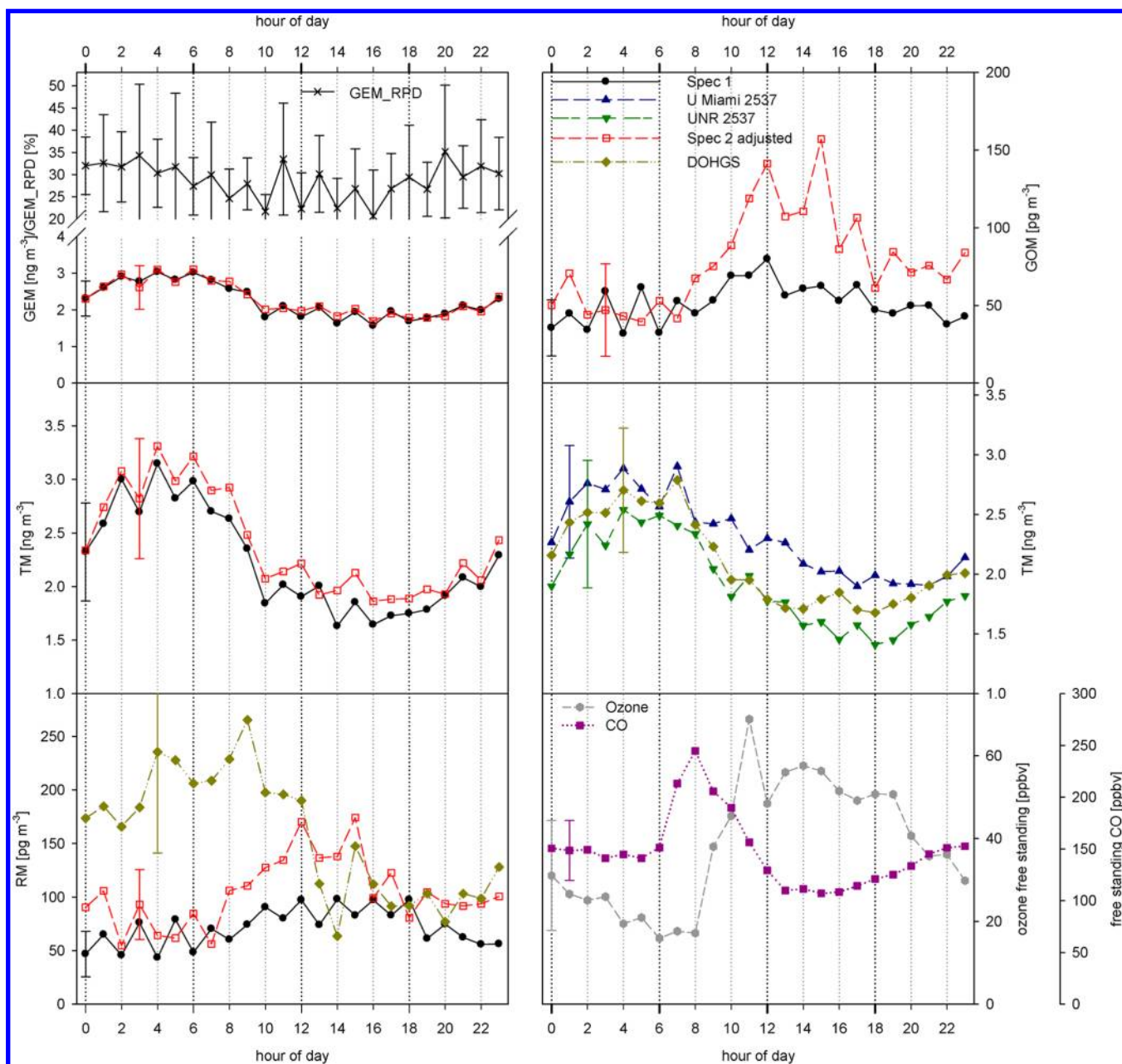


**Figure 2.** Diel bin plots of mean GEM, GOM, TM (GEM + GOM + PBM), and RM (GOM + PBM), concentrations measured directly from the manifold. No spike data are included. Spec 2 adjusted represent the measurements by Spec 2 divided by 0.72. GEM\_RPD is the relative percent difference between the Spec 1 and Spec 2 GEM data. The error bar indicates 1 standard deviation. Free standing CO and O<sub>3</sub> data are also presented. The order of the legend and the error bars correspond to the order of these instruments in the manifold.

(Figure 1, for details see SI, Table SI 1). The protocol developed for the Tekran system by the Atmospheric Mercury Network (AMNet) of the National Atmospheric Deposition Network (NADP)<sup>15</sup> was applied with differences described below. Because a cyclone was attached to the inlet of the manifold system to remove particulate matter larger than 1  $\mu\text{m}$ , the Tekran elutriator, designed to remove those larger than 2.5  $\mu\text{m}$ , was replaced with 1.5 m of Teflon PFA tubing (1.27 cm O.D.). This tubing was connected to the manifold with a Teflon National Pipe Thread tapered head fitting. This connection and the glass inlets to the Tekran 2537/1130/1135 systems were heated to 100  $^{\circ}\text{C}$ . With this setting, when the air entered the Tekran 1130/1135 unit, a temperature drop of 50  $^{\circ}\text{C}$  occurred. Due to the competition between the

manifold and Tekran system pumps, and the low atmospheric pressure associated with the high elevation of Reno (1340 m), these two units were operated at 4 L min<sup>-1</sup> instead of the 10 L min<sup>-1</sup> suggested. The lower flow rate would not significantly affect denuder performance based on the capture efficiency calculated using the equation in Allegrini et al.<sup>31</sup> The UNR-operated 2537 unit sampling line included a 0.2  $\mu\text{m}$  pore size Teflon filter, and was 5 m long, covered, and heated to 50  $^{\circ}\text{C}$ . For more details on Tekran operation, configuration, and quality control procedures, see the SI.

The University of Miami operated a Tekran 2537 unit and a Laser Induced Fluorescence (LIF) system for the measurement of GEM.<sup>32</sup> The former sampled through 7.6 m of uncovered Teflon tubing with a 0.25  $\mu\text{m}$  pore size particle filter in-line



before the air entered the analyzer. Air entering this unit was cooled to 20 °C as it entered the sampling trailer.

The DOHGS system operationally quantifies TM and GEM using two Tekran 2537 units. The TM measurement was made by pulling air through a quartz tube (2.2 cm diameter  $\times$  17.2 cm long) packed with quartz wool and heated to 650 °C, while the GEM measurement was made by pulling the air through a quartz wool packed trap at  $\sim$ 25 °C.<sup>33</sup> This data is applied to calculate reactive Hg (RM = GOM + PBM) by subtracting the GEM measurement from the TM measurement.

The UHMERC instrument applies the same general collection and analyses method as the Tekran system,<sup>34</sup> and measured GEM during the first week of the experiment. This instrument was connected to the manifold using a custom Teflon port connection that sampled air from the center of the manifold. The inlet to this instrument included 1.5 m of Restek Silco-Steel Sulfinert tubing heated to 50 °C. A Teflon filter was situated at the sample inlet to remove fine particles ( $<2\ \mu\text{m}$ ) with a molecular sieve trap immediately after to remove GOM. Gold traps in CVAFS analyzers were heated to 460 °C.

During the first two weeks of the experiment UNR collected Hg on nylon membranes (0.2  $\mu\text{m}$ ; P/N EW-36229-04, Cole Parmer). Samples were collected for 24 to 48 h on top of the trailer housing the Tekran 2537/1130/1135 systems four times during the first two weeks of the study (for details see SI and ref 28).

Detection limits for GOM as measured by the Tekran 1130 unit using dry clean air were  $\sim$ 10  $\text{pg m}^{-3}$  (see SI) and for the DOHGS unit was 50  $\text{pg m}^{-3}$  at TM concentrations of 1.5  $\text{ng m}^{-3}$  and 70  $\text{pg m}^{-3}$  at a mean TM concentration of 2.4  $\text{ng m}^{-3}$  (cf. ref 33). The GEM detection limit is 0.1  $\text{ng m}^{-3}$  as specified by Tekran Instrument Corporation.

**Data Analyses.** Estimated percent spike recoveries ( $\text{ES}_{\text{recovery}}\%$ ) during RAMIX are calculated using data collected simultaneously by one free-standing Tekran system ( $C_{\text{fs}}$ ) and one connected to the manifold ( $C_{\text{m}}$ ). Recoveries were calculated using hourly averaged concentrations. Because transmission efficiencies of Hg through the manifold were not field tested, spike concentrations are based on the spike amounts and flow rate ( $C_{\text{spike}}$ ) (see SI for details). The equation applied was as follows:

$$\text{ES}_{\text{recovery}}\% = ((C_{\text{m}} - C_{\text{fs}})/C_{\text{spike}}) \times 100 \quad (1)$$

During Week 3, estimated spike responses ( $\text{ES}_{\text{response}}\%$ ) were calculated using the mean hourly concentrations measured during the spikes ( $C_{\text{m at } t=0}$ ) minus the ambient manifold concentration measured the previous hour ( $C_{\text{m at } t=-1}$ ), divided by  $C_{\text{spike}}$ .

$$\text{ES}_{\text{response}}\% = ((C_{\text{m at } t=0} - C_{\text{m at } t=-1})/C_{\text{spike}}) \times 100 \quad (2)$$

Relative percent difference (RPD) was calculated using concentrations measured by a reference instrument ( $C_{\text{RI}}$ ) and the one of interest ( $C_{\text{II}}$ ) as follows,

$$\text{RPD}\% = ((C_{\text{RI}} - C_{\text{II}})/C_{\text{RI}}) \times 100 \quad (3)$$

The reference instruments for GEM and RM were Spec 1 and DOHGS, respectively.

Statistical analyses were done using Minitab v16 (Minitab Inc., State College, Pennsylvania) and SigmaPlot v11 (Systat Software, Inc., Chicago, IL). For additional description of data analyses, see SI.

## RESULTS AND DISCUSSION

**Setting the Stage.** Overall, atmospheric chemistry at MDN NV98 will be influenced by planetary boundary layer (PBL) height, inputs from the free troposphere, nearby agricultural activities, roadways, and industry (cf. ref 30). During RAMIX, two fronts moved through the area and influenced overall atmospheric chemistry (Figures SI 1–5). A stable high pressure system persisted during Weeks 1 and 2. At the end of Week 2, a low pressure system moved into the area. A new system moved into the area at the end of Week 3, bringing precipitation across the area. As a result, higher mean relative humidity (RH) was observed during Week 4 than Weeks 1 to 3 ( $\sim$ 40 to 50% versus 30%, Figure SI 2).

All instruments applied during RAMIX were operated under a stringent set of quality control procedures, as defined by each research team for their respective systems (see SI and the corresponding refs 27 and 32–34). Additionally, each sampling method, as applied, had a unique configuration with respect to data collected. Lastly, all measurements were made using ambient air, and previous tests of a similar manifold were made in the laboratory.<sup>27</sup>

**Data Comparisons. Tekran 2537/1130/1135 Measurements.** Comparison of Tekran 2537/1130/1135 data (including: manifold, free-standing, and during spikes; Table SI 2, Figures SI 6 and 7) showed systematically lower GEM and TM concentrations (GEM + GOM + PBM) measured by Spec 2. Despite repeated calibrations and quality assurance measures, this bias persisted throughout the experiment. Additionally, the RPD between mean hourly GEM concentrations, measured by Spec 1 and 2, consistently showed the latter to be lower by 25 to 35% (Figure 2). Because of this, the data collected using Spec 2 was adjusted based on the relationship between this unit and Spec 1 collected during the GEM spikes [ $\text{Spec 2 (GEM ng m}^{-3}) = 0.72 \times \text{Spec 1} + 0.08$ ;  $r^2 = 0.89$ ,  $n = 149$ ,  $p < 0.001$ ] (Figure SI 6). Thus, Spec 2 data are divided by 0.72 and described as “Spec 2 adjusted” from here on.

Application of this adjustment factor resulted in comparable mean GEM concentrations overall measured by the two Tekran systems, when they were free-standing (Table SI 2). Application of this factor, however, resulted in the mean GOM and PBM concentrations for Spec 2 adjusted being higher than that calculated for Spec 1 when in-the-manifold (by 30 and 10  $\text{pg m}^{-3}$ , respectively), but not when free-standing. The same two denuders, coated by the same operator, were used from Sept 2 to 13, and these were switched between instruments on September 9. Prior to switching the slope for the equation comparing GOM as measured by Spec 1 versus Spec 2 adjusted was 1.7 ( $r^2 = 0.57$ ,  $p < 0.5$ ,  $n = 76$ ) after switching this was 1.2 ( $r^2 = 0.62$ ,  $p < 0.05$ ,  $n = 42$ ). This indicates that although there may have been some systematic bias between denuders Spec 2 adjusted consistently measured more GOM than Spec 1. We hypothesize that this trend is due to production of RM in the manifold (discussed later).

**Spike Recoveries.** Using the Tekran 2537/1130/1135 data, and applying the Spec 2 adjustment factor, mean GEM  $\text{ES}_{\text{recovery}}\%$  obtained during Week 4 was  $76 \pm 7\%$ , and GEM  $\text{ES}_{\text{response}}\%$  for Weeks 1 to 3 were 76, 72, and 76% as measured by the UNR 2537 unit, Spec 1, and Spec 2 adjusted, respectively (Table SI 3). These units were situated in this order moving down flow in-the-manifold (Figure 1). Combining these over the entire RAMIX campaign, the  $\text{ES}_{\text{recovery/response}}\%$  for Spec 1 (that was in-the-manifold over all

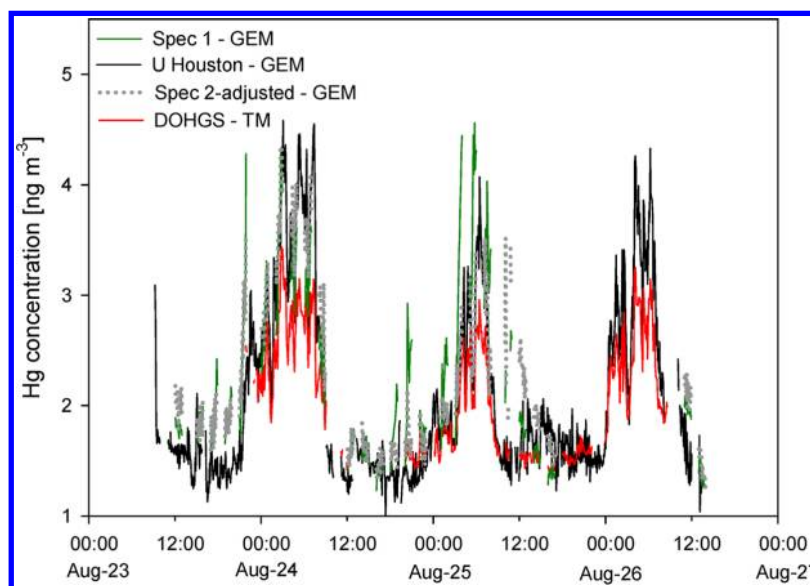


**Figure 3.** GEM as measured by Spec 1, University of Houston and Spec 2-adjusted, and TM as measured by the DOHGS during the Week 1.

weeks) for spike concentrations that ranged from 5 to 25 ng m<sup>-3</sup> was 78% ( $r^2 = 0.87$ ,  $p < 0.001$ ,  $n = 23$ ).

The DOHGS GEM ES<sub>response</sub>% was  $81 \pm 4\%$ <sup>33</sup> while that for the UHMER instrument obtained during Week 1 ( $n = 3$  h) was  $91 \pm 10\%$  (Spec 1 and Spec 2 adjusted responses during Week 1 were  $83 \pm 5\%$  and  $75 \pm 8\%$ ; respectively). The higher response by the UHMER instrument was due to either better detection of GEM based on the sampling configuration, or an artifact of their sampling location within the manifold.

Because of the manifold inlet, it cannot be assumed that all Hg in ambient air entering the manifold was gaseous. Additionally, the fact that PBM was measured by the Tekran systems suggests that this form, or one not captured by the denuder, was present. At the temperature of the manifold ( $115 \pm 2$  °C), and considering gas particle partitioning coefficients for divalent Hg,<sup>13,35</sup> ~99% of Hg in-the-manifold should have been in the gas phase. However, chemistry of the air, the aerosols, and RM at the site are unknown.

Because it has been suggested that sampling artifacts for the Tekran system exist, with GOM being collected on the PBM unit<sup>36,37</sup> (see SI for details), PBM and GOM were combined as RM to assess the HgBr<sub>2</sub> spike recoveries, and to compare with data collected by the DOHGS. The HgBr<sub>2</sub> ES<sub>recovery</sub>% calculated using the Tekran data collected for Week 4 was  $17 \pm 3\%$  ( $n = 18$ , Table SI 3). Week 3 HgBr<sub>2</sub> spike responses were  $23 \pm 13\%$  and  $33 \pm 22\%$  for Spec 1 and Spec 2 adjusted, respectively. This suggests a low recovery by the denuder and/or loss of the spike as it moved through the manifold. If the latter, given the residence time of air in-the-manifold (~1.5 s), then this suggests that fast reactions were occurring. During times when HgBr<sub>2</sub> was spiked, Spec 2 adjusted measured more GOM than Spec 1 (Spec 2 adjusted GOM concentration (pg m<sup>-3</sup>) =  $2 \times$  Spec 1 (pg m<sup>-3</sup>) - 8 (pg m<sup>-3</sup>);  $r^2 = 0.57$ ,  $n = 18$ ,  $p < 0.05$ ).

During HgBr<sub>2</sub> spikes in Week 3, RPDs for RM measured by Spec 1 and Spec 2 adjusted versus the DOHGS were  $54 \pm 23\%$  and  $45 \pm 25\%$ , respectively. If this is done for Week 4, using the Spec 1 data only, RPD was  $74 \pm 8\%$  (Figures 2 and SI 12). During Week 4 the highest relative humidity was measured (~40 to 50% versus 30%), and as suggested by Landis et al.<sup>38</sup> and Feng et al.,<sup>39</sup> it is possible that hydrolysis of the KCl denuder was inhibiting spike recovery.

### Assessment of Hg Transmission in-the-Manifold.

During RAMIX, five Tekran systems measured operationally defined TM concentrations: the two Tekran 2537/1130/1135 systems, the University of Miami and UNR 2537 instruments, and the DOHGS system. Linear regression analyses comparing all TM data (spikes and no spikes) collected by the University of Miami 2537 as  $x$  and DOHGS units as  $y$  (located at the front and end of the heated component of the manifold, respectively), yielded a regression analysis slope of 1.0 and an intercept of  $0.1 \text{ ng m}^{-3}$  ( $r^2 = 0.98$ ,  $p < 0.01$ ), the detection limit of the Tekran 2537 unit, indicating that these two instruments were in good agreement (Table SI 4). We hypothesize that long exposed Teflon line connected to the University of Miami Tekran 2537 unit provided a setting that promoted conversion of RM to GEM, or that RM was transported efficiently through this line and quantified by the Tekran system. The latter seems unlikely given the system configuration, and range in vapor pressures of GOM compounds (cf. ref 8). Comparison of the University of Miami 2537 data ( $x$ ) versus the DOHGS GEM data ( $y$ ), not including the spike data, also supports the first hypothesis (slope of 0.5, intercept of  $0.92 \text{ ng m}^{-3}$ ,  $r^2 = 0.53$ ,  $p < 0.05$ ). The slopes for regression equation comparing all the University of Miami 2537 data ( $x$ ) with Spec 1 and Spec 2 adjusted TM data was  $1 \pm 0.02$  (Table SI 4) also indicating good transmission through the manifold.

Comparing TM data collected by the UNR 2537 unit ( $x$ ) with that measured by the other instruments yielded intercepts that ranged from 0.4 to  $0.6 \text{ ng m}^{-3}$  (Table SI 4). Reactive mercury concentrations of these amounts were measured by the DOHGS unit during RAMIX. The systematic bias between the UNR 2537 data and that collected with the other instruments, likely reflects a "loss" of RM in the line due to the temperature drop of 50 °C, and insulation of this line, between the manifold and the UNR 2537 unit. An alternate hypothesis is that the RM may have been collected on the soda lime and  $0.2 \mu\text{m}$  particulate filter; however, prior work at this field site has shown this is not the case (see summary in ref 26). This hypothesis is supported by the agreement between the UNR 2537 ( $x$ ) and the DOHGS GEM data ( $r^2 = 0.75$ ,  $p < 0.05$ ). Additionally, the UM LIF method only measures GEM, and data collected with this instrument did not correlate well

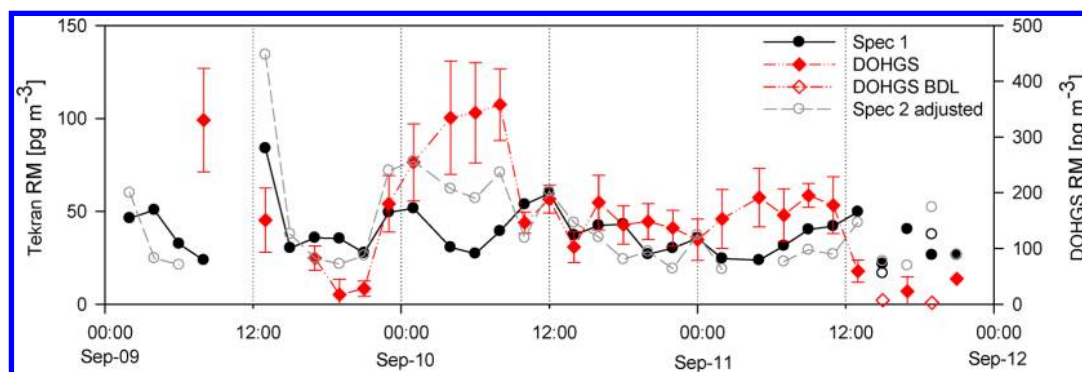


**Figure 4.** Hourly mean RM concentrations measured by Tekran Spec 1, Spec 2, Spec 2 adjusted (Spec 2 data divided by 0.72) and DOHGS. BDL indicates below instrument detection limit.

with that collected by the University of Miami 2537 unit but showed a good correlation with the UNR 2537 observations (data not shown; Anthony Hynes, personal communication).

The above hypothesis is also supported by comparison of all 24-h trends in mean hourly TM (Figure 2). The UNR 2537 unit measured consistently the lowest concentrations, and the University of Miami 2537 the highest during the day. Additionally, a decline in mean hourly TM from night-to-day occurred for all systems with the greatest difference occurring in the afternoon. If data derived using UNR 2537 unit reflects the diel change in GEM at the site, and the University of Miami the TM coming into the manifold, then  $\sim 0.5 \text{ ng m}^{-3}$  of RM was not being measured by the UNR 2573. The intercepts for the regression equations comparing the UNR 2537 unit with the others collectively indicate  $\sim 400$  to  $600 \text{ pg m}^{-3}$  of RM were not being measured (Table SI 4).

**Trends over Time. Ambient Measurements.** Free-standing GEM, GOM, and PBM concentrations (median Spec 1:  $2.2 \text{ ng m}^{-3}$ ,  $23 \text{ pg m}^{-3}$  and  $7 \text{ pg m}^{-3}$ ; respectively; Table SI 2) were similar to those reported in previous work at this same location (Summer and Fall:  $2.1 \text{ ng m}^{-3}$ ,  $20 \text{ pg m}^{-3}$  and  $8 \text{ pg m}^{-3}$ ; respectively; <sup>30</sup>). Gaseous elemental Hg concentrations measured in-the-manifold were comparable to free-standing and previous data; however, for both Spec 1 and 2 adjusted, GOM and PBM data collected while sampling from the manifold were higher (Table SI 2). GEM concentrations measured during the Week 1 by the UHMERC instrument were lower in general than those measured by Spec 1 and Spec 2 adjusted ( $y$ ) (slopes of 0.64 and 0.89, intercepts of  $-0.50$  and  $0.57 \text{ ng m}^{-3}$ , and  $r^2$  of 0.56 and 0.77,  $p < 0.01$ ,  $n = 170$  and 169; respectively; Figure 3), and at time greater than DOHGS measured TM.

Replicate nylon membranes deployed during Weeks 1 and 2 collected 30 to 50% more RM than Spec 1 (Table SI 5). Additional work at this site showed that cation exchange membranes collected more RM than that measured by the nylon membranes and the Tekran system.<sup>28</sup> This is supported by recent work using passive sampling systems that showed forms of RM are present that are not measured by the Tekran system.<sup>40</sup> Additionally, the range in desorption temperatures for RM from the nylon membranes was 100 to  $160^\circ\text{C}$  (data not shown). Since the manifold was maintained at  $\sim 100^\circ\text{C}$  this suggests that RM could have been deposited to the manifold surface. The affinity of different forms of RM is also likely to be different for different surfaces, i.e. Teflon, nylon, and glass.<sup>28,41,42</sup>

Higher GEM concentrations measured at night are due to local-source emissions into a shallow boundary layer (cf. ref 30). On the basis of data collected when both Tekran systems were free-standing, GEM was negatively correlated with GOM ( $r = 0.43$  and  $0.58$ , Spec 1 and Spec 2 adjusted;  $p < 0.05$ ); significantly negatively correlated with  $\text{O}_3$  and temperature ( $r > 0.7$ ); poorly correlated with CO; and strongly correlated with relative humidity ( $r = 0.8$ ). Gaseous oxidized Hg was significantly positively correlated with  $\text{O}_3$  ( $r = 0.65$ ), temperature ( $r = 0.65$ ), and solar radiation ( $r = 0.37$  to  $0.45$ ), and negatively correlated with relative humidity ( $r = 0.75$ ). These results suggest local production of GEM during the night and GOM during the day (Table SI 6).

On most days a significant increase in mean hourly  $\text{O}_3$  concentrations was observed from 0800 to 1100 h (Figure 2). After 1100 h, concentrations decreased and remained fairly constant at 45 ppbv throughout the afternoon (Figure 2). Over this time modeled PBL height also showed a dramatic increase (from 100 to 1000 m above ground level; Figure SI 1). Carbon monoxide concentrations increased from 0600 to 0800 h when wind speeds were lowest and direction shifted from south to west, and then declined reaching a minimum in late afternoon (Figure 2; Figures SI 4 and SI 5). Ozone and CO concentrations were negatively correlated; however, this relationship only explained  $\sim 50\%$  of the variance (Table SI 6). Carbon monoxide was positively correlated with RH, explaining 45% of the variability. This suggests that some CO, but not all, was due to local pollution. For more than 50% of the days during Weeks 1, 2, and 4, a secondary peak in the 5-min CO was observed at  $\sim 1100$  h (detailed data not shown). The high CO concentrations in the morning reflect inputs to a shallow boundary layer from vehicle traffic on a nearby heavily traveled roadway. The peaks of CO,  $\text{O}_3$ , and GOM (Figure 2) in the late morning reflect mixing of polluted parcels of air to the surface from the free troposphere (cf. ref 43).

The highest in-the-manifold values of GOM ( $400 \text{ pg m}^{-3}$ ) were measured by the Tekran systems at the start of the experiment (Figure SI 8). Since new tubing was used for the manifold, this is thought to be due to flushing of contamination as the tubing was heated. Over the experiment both systems measured higher GOM ( $50$  to  $200 \text{ pg m}^{-3}$ ) in the afternoon and at times these were greater for Spec 2 adjusted data by 50 to  $100 \text{ pg m}^{-3}$ . This suggests that during the day a form of GOM was being produced in-the-manifold that was not being measured by Spec 1 (cf. Figure 2 and Figures SI 8 and 9).

Concentrations of PBM were higher and more variable during Weeks 1 and 2 ( $25$  to  $100 \text{ pg m}^{-3}$ ) relative to Weeks 3



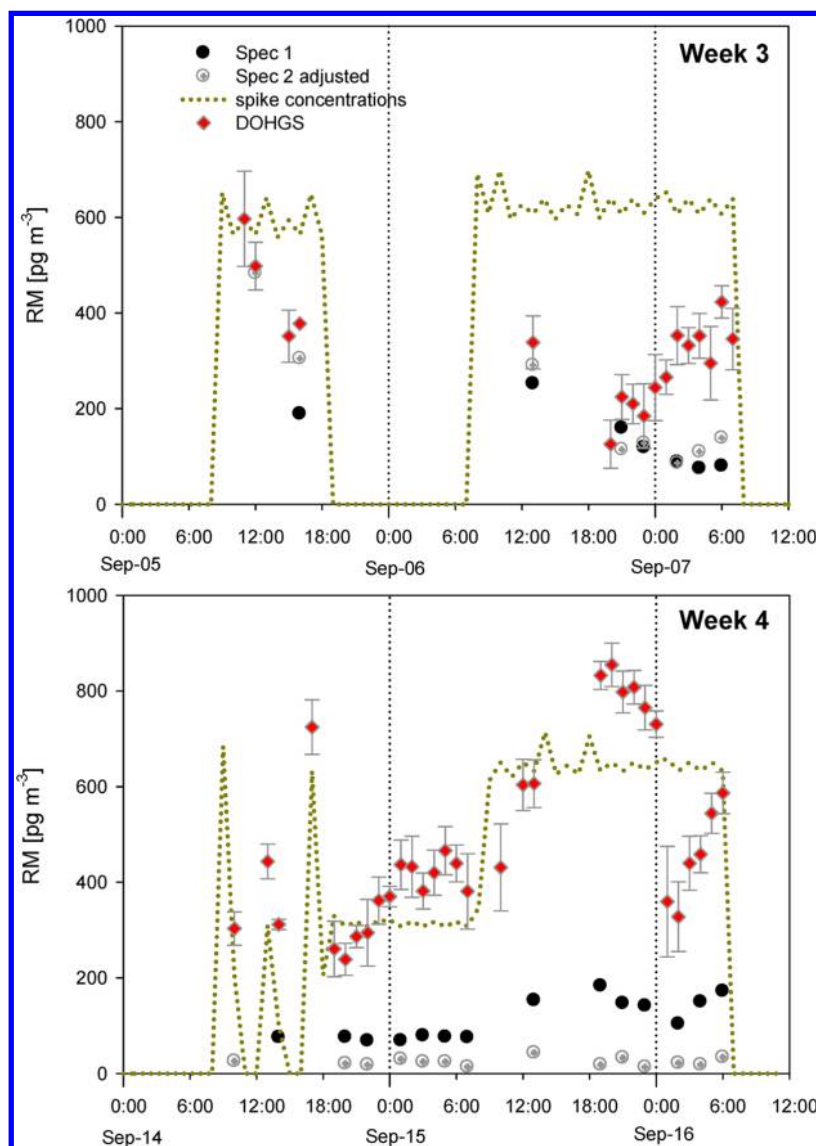


**Figure 5.** Hourly mean RM concentrations measured by the Tekran speciation systems and DOHGS during  $\text{HgBr}_2$  spikes. In the upper panel, during Week 3 both Spec 1 and 2 were sampling from the manifold. In the lower panel, that shows Week 4 data, only Spec 1 was sampling from the manifold. Speciation 1 and 2 data represent a single hourly measurement. The error bar on DOHGS data represents 1 standard deviation.

and 4 ( $<25 \text{ pg m}^{-3}$ ). During this time, wildfires were in the Carson City, Nevada area (50 km, south), and the Sierra Nevada Mountains (100 km, south)<sup>44</sup> and the predominant wind direction during this period was from the south (50%, 135 to 225°). Given the high pressure system occurring at this time it is likely that air aloft was being circulated to the ground. Previous studies have reported high PBM concentrations associated with wildfires.<sup>45,46</sup>

During Weeks 1 and 2,  $\sim 4$  ppbv higher  $\text{O}_3$  concentrations were measured in-the-manifold. This was not an instrument bias because side-by-side comparisons at the beginning, middle and end of the experiment showed 1.4, 0.6, and 0 ppbv differences between these instruments (respectively; see SI for details). During Weeks 1 and 2, PBM concentrations were higher for Spec 2 adjusted (Figure SI 8 and 9). Additionally, the daytime PBM peak concentration occurred roughly at 1100 h corresponding with peak  $\text{O}_3$  concentrations hypothesized to reflect down mixing from the free troposphere. Input from the free troposphere has been suggested to be an important source

of RM in wet and dry deposition measured in Nevada.<sup>22,30,43,47–49</sup>

The continued higher RM and GOM concentrations measured by the Tekran systems over the course of the day suggests local production since wind speeds increased and this would have diluted concentrations. That higher RM was measured by Spec 2 adjusted relative to Spec 1 ( $\sim 100 \text{ pg m}^{-3}$ ) during the day and night supports the hypothesis that RM was being produced in-the-manifold.

The DOHGS system measured significantly more RM at night relative to the Tekran systems (Figure 4). During the night, the boundary layer was shallow, stagnant, and impacted by the sheep housing facility and other nearby agricultural activities. Since the nighttime elevated PBM concentrations were not measured by Spec 1, we suggest that reactions associated with aerosols and surfaces and/or gas phase reactions with nitrogen compounds were forming a RM compound that was not being collected by the Tekran system but was measured by the DOHGS system (Figure 2). The high relative humidity at night could also impact observations (cf. ref

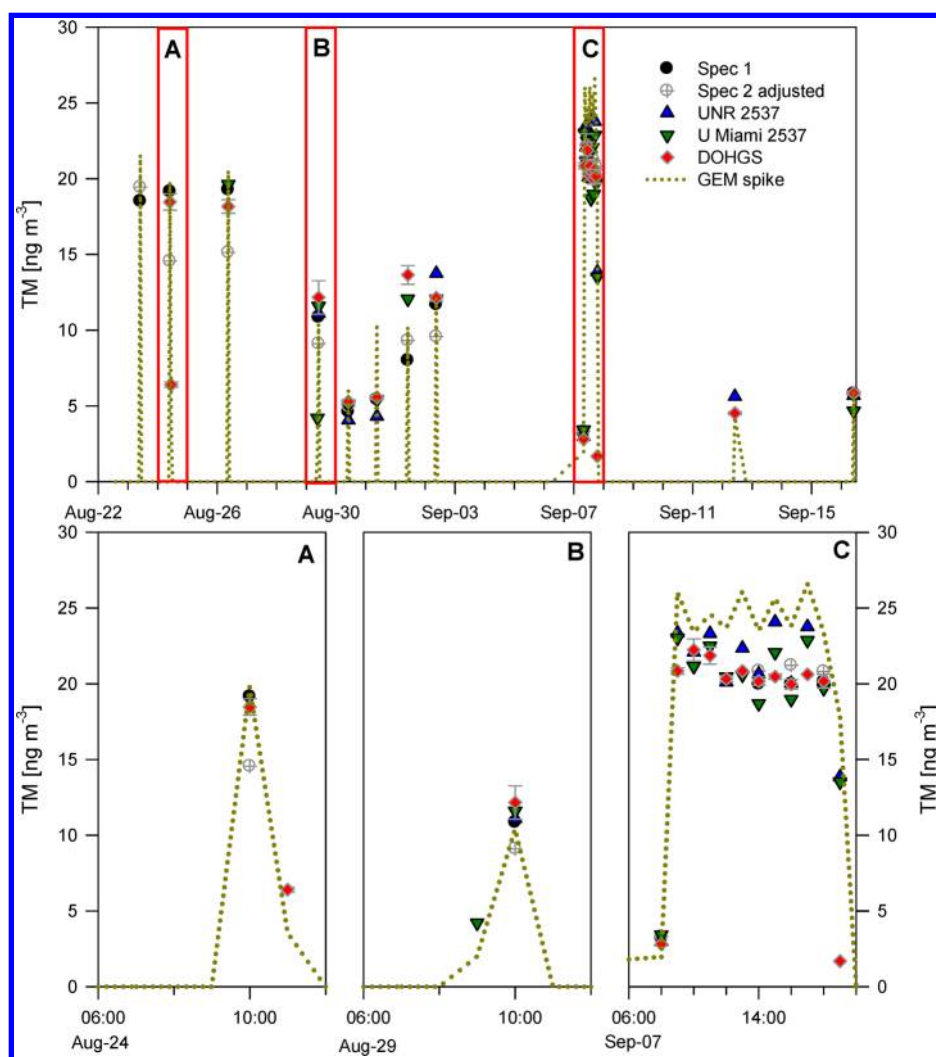


**Figure 6.** Hourly mean TM concentrations measured from the manifold for five systems during GEM only spikes. Due to multiple spikes at times A, B, and C, the data are shown in detail in the bottom panel. Only the DOHGS measured TM August 24 at 11:00, and only the University of Miami measured TM August 29 at 9:00. There is no Spec 1 data in panel C due to inlet leaks in the afternoon. Tekran derived data points represent a one hour measurement while the DOHGS data mean values and one standard deviation.

50). Noteworthy is the fact that during Weeks 1 and 2, when the Tekran systems were out of line, the high PBM concentrations were not observed at night (cf. Figures SI 8 and 9) supporting our hypothesis that RM was being produced in-the-manifold. In summary, during the day RM was being generated locally at the field site and in the manifold, and input to the site by way of the free troposphere; and during the night it was being generated locally and in the manifold.

In contrast to data collected in Weeks 1 and 2, Week 3 PBM concentrations were greater for Spec 1 than Spec 2 (Figure SI 10). Due to the low pressure system, during this week, the PBL height was higher than other weeks. Mean daily and peak CO concentrations were also high relative to other weeks (Figure SI 3). During this time, a form of RM was deposited to the Tekran particulate unit associated with Spec 1 but lost in-the-manifold prior to reaching Spec 2.

During Week 3, diel GOM concentrations declined relative to previous weeks and did not increase during Week 4 after the denuders were changed (Figure SI 11). The decrease in concentrations measured during Week 3, occurred after a water vapor spike on Sept 8th, but could be attributed to the general field conditions, as a low pressure system (that increased the

PBL height) moved out of this area at the end of Week 3. The highest RH was measured during Week 4 (Figure SI 2). Although sampling for RAMIX officially ended September 16th, UNR made free-standing measurements through the 19th. From the 17th to 19th, the RH decreased (50 to 40%) and the GOM and PBM concentrations only increased slightly (Figure SI 11). These observations could be explained by hydrolysis of the KCl coating, as suggested by Landis et al.<sup>38</sup> and Feng et al.,<sup>39</sup> or simply, less GOM in the air during time periods of high RH. This needs to be further investigated.

**HgBr<sub>2</sub> Spikes over Time.** During the first HgBr<sub>2</sub> spike that occurred Week 3, RM as measured by the Tekran and DOHGS systems declined over the course of the day (Figure 5; see ref 33 for details). This is in contrast to observed ambient RM concentrations that generally increased over the course of the day (Figure 5). During the second HgBr<sub>2</sub> spike (September 6th to 7th; Figure 5), concentrations as measured by the Tekran and DOHGS systems were comparable to those measured at the same time the previous day. These instruments reported ~200 and 400 pg m<sup>-3</sup>, respectively, while the estimated spike concentration was ~600 pg m<sup>-3</sup>. Overnight, Tekran measured



concentrations were low and stable, while the DOHGS instrument exhibited increasing concentrations (Figure 5).

During Week 4, when only Spec 1 was measuring in-the-manifold, RM concentrations measured by this instrument were low and stable across time for two different  $\text{HgBr}_2$  concentrations; however, the DOHGS instrument derived values were both higher and lower than the spike concentration (Figure 5). Specifically, during the lower concentration spike (September 14th and 15th at  $400 \text{ pg m}^{-3}$ ), that occurred overnight, Tekran measured GOM concentrations were  $75 \text{ pg m}^{-3}$  and there was little PBM, while the DOHGS instrument measured  $\sim 100$  to  $400 \text{ pg m}^{-3}$  higher RM. During the day of September 15th, the spike concentration was increased to  $600 \text{ pg m}^{-3}$  and GOM and PBM concentrations measured by the Tekran system increased by  $\sim 50 \text{ pg m}^{-3}$ . During this spike, DOHGS measured RM was  $600 \text{ pg m}^{-3}$  during mid-day and  $800 \text{ pg m}^{-3}$  at night. This indicates that: (1) there was significantly more RM measured by the DOHGS than by the Tekran system, and (2) different forms of RM were present in the atmosphere.

During most  $\text{HgBr}_2$  spikes, PBM concentrations increased significantly for Spec 1 but not for Spec 2 (Figures SI 10 and 11). This suggests incomplete capture by the denuder of added GOM and loss of the spike in-the-manifold. The nighttime increases in the DOHGS unit RM concentrations, were positively correlated with RH (see ref 33 for details).

The low RM daytime spike responses during the day by both the Tekran and DOHGS instruments during Week 3 relative to Week 4 (Figure 5) could reflect a systematic change in air chemistry affecting the spike, or an analytical artifact associated with the gold trap used to quantify GEM by both systems or the quartz trap used to scrub GOM by the DOHGS system.<sup>33</sup> For example, some work has suggested that  $\text{O}_3$  could influence the ability of the gold surface to collect GEM.<sup>51</sup> The latter, however, seems unlikely since a GEM spike over the day did not show a decreasing trend (Figure 6).

**Implications.** Given the systematic Tekran 2537/1130/1135 instrument differences, and despite passing intensive quality control checks, unless these instruments are compared with a common unit, observations may not be applied for assessing spatial and temporal variations.

On the basis of ambient and spike recovery and responses, the KCl-coated denuder as currently applied does not efficiently collect  $\text{HgBr}_2$  and other RM compounds that occurred in the air during RAMIX. Huang et al.<sup>28</sup> also demonstrated that  $\text{HgBr}_2$ ,  $\text{HgCl}_2$ , and  $\text{HgO}$  concentrations measured using nylon and cation exchange membranes were 1.6 to 3.7 times higher than that measured using KCl coated denuders and these forms are not similarly captured by the denuder surface.

Analyses of operationally defined TM measurements showed that atmospheric Hg was being transferred through the manifold, but the Tekran systems and the UNR 2537 as configured were not measuring all RM. Results indicate that covered Teflon tubing (not typically used for Hg measurements), and decreases in temperature will facilitate in-line RM deposition.<sup>17</sup> Teflon tubing is not recommended for particulate matter sampling due to static electricity.<sup>52</sup> On the basis of data comparisons, we suggest that the manifold and sampling lines provided a setting where forms of RM could be deposited. These observations have implications for designing Hg measurement systems.

Data point toward different forms of RM being present in the local atmosphere and being produced in-the-manifold. A potential mechanism for this could be heterogeneous reactions associated with aerosols containing nitrogen compounds and semivolatile organic compounds<sup>53</sup> or homogeneous reactions influenced by ambient atmospheric chemistry (cf. refs 50, 54 and references therein). Also, aerosol based semivolatile organic compounds have reactive oxygen associated.<sup>55</sup> However, given the uncertainties associated with the chemistry of the air entering the manifold and the heterogeneous surfaces, we can only speculate on this.

The lack of recovery of the  $\text{HgBr}_2$  spike suggests manifold reactions were removing this form before reaching the instruments. However, measurements by the DOHGS system quantified  $\sim 80\%$  of the  $\text{HgBr}_2$  spikes at times and measured much higher RM. On the basis of known vapor pressures, Lin et al.<sup>5</sup> pointed out that  $\text{HgCl}_2$  would “remain in the gas phase long enough to be detected”; however, the same may not be true for  $\text{HgBr}_2$ .

Lin et al.<sup>5</sup> suggested that based on the wide range in reported vapor pressures for  $\text{HgO}$ , this form could exist at concentrations ranging from  $0.7$  to  $200 \text{ pg m}^{-3}$  and would exist as a solid phase. Experimental work by Pal and Ariya<sup>56</sup> showed that  $\text{HgO}$  could be produced by reactions with  $\text{O}_3$  with only a small amount (1%) measured on an aerosol filter. Calculations based entirely on theory suggest that if produced,  $\text{HgO}$  would not exist as an isolated molecule. Once produced, this form could be deposited to and retained by the manifold given that the temperature of decomposition is  $+500^\circ\text{C}$ .<sup>8</sup> However, the presence of other gases in ambient air might influence the reactions and the decomposition temperature.<sup>50,54,57,58</sup>

The potential for other oxidation reactions cannot be ruled out. Lin et al.<sup>5</sup> mentioned that other gaseous oxidants such as  $\text{NO}_3$ ,  $\text{HO}_2$ ,  $\text{O}^1\text{D}$ ,  $\text{O}^3\text{P}$ , etc. may be important. Seigneur et al.<sup>58</sup> also suggested a variety of heterogeneous reactions. It is important to note that there are not reaction rates for all forms of GOM and those available are based on theory and limited empirical data involving simple systems. Only recently have data been collected in laboratory conditions that attempt to simulate complex ambient air chemistry.<sup>50,54</sup>

Collectively, the data showed that RM concentrations could be 2-to-3-fold higher than that reported in the literature.<sup>1</sup> This indicates that dry deposition as predicted by those using denuder-derived data and models would be underestimated. This has significant implications for policy makers involved with protecting humans and wildlife from Hg contamination. Cumulatively, data showed that local, regional, and global atmospheric chemistry were influencing Hg measured at the RAMIX field site. Without understanding the chemistry of RM compounds, and the homogeneous and heterogeneous processes association with formation and destruction, we cannot adequately assess the limitations of the instruments applied during RAMIX or the sources. Our understanding of atmospheric Hg is also hampered by our understanding of the chemistry of the atmosphere which, as demonstrated by a multitude of papers presented at the December American Geophysical Union meeting, is still a work in progress. Comparison of our results with those obtained using chemical transport models could help us better understand these processes.

## ■ ASSOCIATED CONTENT

### ■ Supporting Information

12 pages of text, 6 Tables, and 12 Figures. This material is available free of charge via the Internet at <http://pubs.acs.org>.

## ■ AUTHOR INFORMATION

### Corresponding Author

\*Phone: 1-775-784-4203; e-mail: [mgustin@cabnr.unr.edu](mailto:mgustin@cabnr.unr.edu).

### Present Address

◆Bingham Research Center, Utah State University Office of Commercialization and Regional Development, 320 N. Aggie Blvd., Vernal, Utah, USA, 84078.

### Notes

The authors declare no competing financial interest.

## ■ ACKNOWLEDGMENTS

This work was funded by the National Science Foundation (Grant No. 1102336). However, it does not reflect the views of the Agency and no official endorsement should be inferred. We thank Tekran Instrument Corp. for discussions while conceiving and during this project, as well as Mark Olson with the National Atmospheric Deposition Program. We thank Dr. Gary Gill for the use of his Tekran Speciation System. Many thanks to Bo Kindred, student support staff at the Nevada Agriculture Experiment Station, and Musheng Alishahi, Travis Lyman, and Vanessa Wehrkamp during this experiment. We also thank the Nevada Division of Environmental Protection for use of two air quality sampling trailers for this project, UNR electricians, Steve Cavallaro and Frank McCarron, for their help and patience, and UNR professor, Bob Nowak for use of his laboratory. We thank the following individuals from the University of Miami who participated in this project for the use of their Tekran 2537 data and providing discussion of comparison of their LIF data: Anthony Hynes, Dieter Bauer, Stephanie Everhart, and James Remeika.

## ■ ABBREVIATIONS

AMNet	Atmospheric Mercury Network
C <sub>fs</sub>	Concentrations measured by free stand system
C <sub>m</sub>	Concentrations measured by the system connected to manifold
C <sub>m</sub> at t=0	Mean hourly concentrations measured during spike
C <sub>m</sub> at t=-1	Ambient manifold concentrations measured prior to spike
C <sub>RI</sub>	Concentrations measured by reference instrument
C <sub>II</sub>	Concentrations measured by interest instrument
C <sub>spike</sub>	Spike concentrations estimated using spike amount and manifold flow rate
CO	Carbon monoxide
CVAFS	Cold Vapor Atomic Fluorescence Spectroscopy
DOHGS	Detector of Oxidized Mercury System
ES <sub>recovery</sub> %	Estimated Percent spike Recoveries
ES <sub>response</sub> %	Estimated Percent spike Response
GEM	Gaseous Elemental Mercury
GOM	Gaseous Oxidized Mercury
Hg	Mercury
LIF	Laser Induced Fluorescence

MDN	Mercury Deposition Network
NADP	National Atmospheric Deposition Program
O <sub>3</sub>	Ozone
O.D.	Outside Diameter
PBL	Planetary Boundary Layer
PBM	Particulate Bound Mercury
PFA	Perfluoroalkoxy
RAMIX	Reno Atmospheric Mercury Intercomparison eXperiment
RH	Relative Humidity
RM	Reactive Mercury
RPD	Relative Percent Difference
SI	Supporting Information
Spec 1	Tekran Speciation system first inline
Spec 2	Tekran Speciation system in second inline
Spec 2 adjusted	Concentrations measured by Spec 2 and corrected by a scaling factor due to the instrumental bias
TM	Total atmospheric Mercury
UHMERC	The University of Houston Mercury instrument
UM	University of Miami
UNR	University of Nevada, Reno
UW	University of Washington-Bothell

## ■ REFERENCES

- (1) Valente, R. J.; Shea, C.; Lynn Humes, K.; Tanner, R. L. Atmospheric mercury in the Great Smoky Mountains compared to regional and global levels. *Atmos. Environ.* **2007**, *41* (9), 1861–1873.
- (2) Ebinghaus, R.; Banic, C.; Beauchamp, S.; Jaffe, D.; Kock, H.; Pirrone, N.; Poissant, L.; Sprovieri, F.; Weiss-Penzias, P. Spatial Coverage and Temporal Trends of Land-Based Atmospheric Mercury Measurements in the Northern and Southern Hemispheres. In *Mercury Fate and Transport in the Global Atmosphere: Emissions, Measurements and Models*; Mason, R., Pirrone, N., Eds.; Springer: New York, 2009.
- (3) Hynes, A. J.; Donohoue, D. L.; Goodsite, M. E.; Hedgecock, I. M. Our Current Understanding of Major Chemical and Physical Processes Affecting Mercury Dynamics in the Atmosphere and at the Air-Water/Terrestrial Interfaces. In *Mercury Fate and Transport in the Global Atmosphere*; Mason, R., Pirrone, N., Eds.; Springer: New York, 2009.
- (4) Ariya, P. A.; Peterson, K.; Snider, G.; Amyot, M. Mercury Chemical Transformations in the Gas, Aqueous and Heterogeneous Phases: State-of-the-Art Science and Uncertainties. In *Mercury Fate and Transport in the Global Atmosphere*; Mason, R., Pirrone, N., Eds.; Springer: New York, 2009.
- (5) Lin, C.-J.; Pongprueksa, P.; Lindberg, S. E.; Pehkonen, S. O.; Byun, D.; Jang, C. Scientific uncertainties in atmospheric mercury models I: Model science evaluation. *Atmos. Environ.* **2006**, *40* (16), 2911–2928.
- (6) Subir, M.; Ariya, P. A.; Dastoor, A. P. A review of uncertainties in atmospheric modeling of mercury chemistry I. Uncertainties in existing kinetic parameters: Fundamental limitations and the importance of heterogeneous chemistry. *Atmos. Environ.* **2011**, *45* (32), 5664–5676.
- (7) Subir, M.; Ariya, P. A.; Dastoor, A. P. A review of the sources of uncertainties in atmospheric mercury modeling II. Mercury surface and heterogeneous chemistry—A missing link. *Atmos. Environ.* **2012**, *46* (0), 1–10.
- (8) Schroeder, W. H.; Munthe, J. Atmospheric mercury—An overview. *Atmos. Environ.* **1998**, *32* (5), 809–822.
- (9) Feng, X.; Lu, J. Y.; Grégoire, C.; Hao, Y.; Banic, C. M.; Schroeder, W. Analysis of inorganic mercury species associated with airborne particulate matter/aerosols: method development. *Anal. Bioanal. Chem.* **2004**, *380*, 683–689.

- (10) Calvert, J. G.; Lindberg, S. E. Mechanisms of mercury removal by  $O_3$  and OH in the atmosphere. *Atmos. Environ.* **2005**, *39* (18), 3355–3367.
- (11) Lindberg, S. E.; Stratton, W. J. Atmospheric mercury speciation: Concentrations and behavior of reactive gaseous mercury in ambient air. *Environ. Sci. Technol.* **1998**, *32* (1), 49–57.
- (12) Seigneur, C.; Abeck, H.; Chia, G.; Reinhard, M.; Bloom, N. S.; Prestbo, E.; Saxena, P. Mercury adsorption to elemental carbon (soot) particles and atmospheric particulate matter. *Atmos. Environ.* **1998**, *32*, 2649–2657.
- (13) Rutter, A. P.; Schauer, J. J. The effect of temperature on the gas-particle partitioning of reactive mercury in atmospheric aerosols. *Atmos. Environ.* **2007**, *41* (38), 8647–8657.
- (14) Tekran, *Model 2537A Mercury Vapour Analyzer User Manual*; Tekran Inc.: Toronto, Ontario, 2001.
- (15) NADP Atmospheric Mercury Network (AMNet) Site Operations Manual. [http://nadp.sws.uiuc.edu/amn/docs/AMNet\\_Operations\\_Manual.pdf](http://nadp.sws.uiuc.edu/amn/docs/AMNet_Operations_Manual.pdf).
- (16) Gustin, M.; Jaffe, D. Reducing the uncertainty in measurement and understanding of mercury in the atmosphere. *Environ. Sci. Technol.* **2010**, *44* (7), 2222–2227.
- (17) Lyman, S. N.; Jaffe, D. A.; Gustin, M. S. Release of mercury halides from KCl denuders in the presence of ozone. *Atmos. Chem. Phys.* **2010**, *10*, 8197–8204.
- (18) Ebinghaus, R.; Jennings, S. G.; Schroeder, W. H.; Berg, T.; Donaghy, T.; Guentzel, J.; Kenny, C.; Kock, H. H.; Kvietkus, K.; Landing, W.; Muleck, T.; Munthe, J.; Prestbo, E. M.; Schneeberger, D.; Slemr, F.; Sommar, J.; Urba, A.; Wallschläger, D.; Xiao, Z. International field intercomparison measurements of atmospheric mercury species at Mace Head, Ireland. *Atmos. Environ.* **1999**, *33* (18), 3063–3073.
- (19) Brown, R. J. C.; Brown, A. S.; Yardley, R. E.; Corns, W. T.; Stockwell, P. B. A practical uncertainty budget for ambient mercury vapour measurement. *Atmos. Environ.* **2008**, *42* (10), 2504–2517.
- (20) Aspmo, K.; Gauchard, P.-A.; Steffen, A.; Temme, C.; Berg, T.; Bahlmann, E.; Banic, C.; Dommergue, A.; Ebinghaus, R.; Ferrari, C.; Pirrone, N.; Sprovieri, F.; Wibetoe, G. Measurements of atmospheric mercury species during an international study of mercury depletion events at Ny-Ålesund, Svalbard, spring 2003. How reproducible are our present methods? *Atmos. Environ.* **2005**, *39* (39), 7607–7619.
- (21) Lyman, S. N.; Gustin, M. S.; Prestbo, E. M.; Marsik, F. J. Estimation of Dry Deposition of Atmospheric Mercury in Nevada by Direct and Indirect Methods. *Environ. Sci. Technol.* **2007**, *41* (6), 1970–1976.
- (22) Peterson, C.; Gustin, M.; Lyman, S. Atmospheric mercury concentrations and speciation measured from 2004 to 2007 in Reno, Nevada, USA. *Atmos. Environ.* **2009**, *43* (30), 4646–4654.
- (23) Steffen, A.; Scherz, T.; Olson, M.; Gay, D.; Blanchard, P. A comparison of data quality control protocols for atmospheric mercury speciation measurements. *J. Environ. Monit.* **2012**, *14* (3), 752–765.
- (24) Temme, C.; Blanchard, P.; Steffen, A.; Banic, C.; Beauchamp, S.; Poissant, L.; Tordon, R.; Wiens, B. Trend, seasonal and multivariate analysis study of total gaseous mercury data from the Canadian atmospheric mercury measurement network (CAMNet). *Atmos. Environ.* **2007**, *41* (26), 5423–5441.
- (25) Slemr, F.; Brunke, E. G.; Ebinghaus, R.; Kuss, J. Worldwide trend of atmospheric mercury since 1995. *Atmos. Chem. Phys.* **2011**, *11*, 4479–4787.
- (26) Gustin, M. S., Exchange of Mercury between the Atmosphere and Terrestrial Ecosystems. In *Advances in Environmental Chemistry and Toxicology of Mercury*; Liu, G., Cai, Y., O'Driscoll, N., Eds.; John Wiley and Sons: New York, 2012.
- (27) Finley, B. D.; Jaffe, D. A.; Call, K.; Lyman, S. N.; Gustin, M. Development, testing, and deployment of an air sampling manifold for spiking elemental and oxidized mercury during RAMIX. *Environ. Sci. Technol.* **2013**, in review.
- (28) Huang, J.; Miller, M. B.; Weiss-Penzias, P.; Gustin, M. S. Comparison of reactive mercury measurements made with KCl-coated denuders, nylon membranes, and cation exchange membranes. *Environ. Sci. Technol.* **2013**, in review.
- (29) Fäin, X.; Moosmüller, H.; Obrist, D. Toward a real-time measurement of atmospheric mercury concentrations using cavity ring-down spectroscopy. *Atmos. Chem. Phys.* **2010**, *10*, 2879–2892.
- (30) Lyman, S. N.; Gustin, M. S. Determinants of atmospheric mercury concentrations in Reno, Nevada, U.S.A. *Sci. Total Environ.* **2009**, *408* (2), 431–438.
- (31) Allegrini, I.; De Santis, F.; Di Palo, V.; Febo, A.; Perrino, C.; Possanzini, M.; Liberti, A. Annular denuder method for sampling reactive gases and aerosols in the atmosphere. *Sci. Total Environ.* **1987**, *67* (1), 1–16.
- (32) Bauer, D.; Campuzano-Jost, P.; Hynes, A. J. Rapid, ultra-sensitive detection of gas phase elemental mercury under atmospheric conditions using sequential two-photon laser induced fluorescence. *J. Environ. Monit.* **2002**, *4* (3), 339–343.
- (33) Ambrose, J. L.; Lyman, S. N.; Huang, J.; Gustin, M.; Jaffe, D. A. Fast time resolution oxidized mercury measurements with the UW detector for oxidized Hg species (DOHGS) during the Reno Atmospheric Mercury Intercomparison Experiment. *Environ. Sci. Technol.* **2013**, in revision.
- (34) Talbot, R.; Mao, H.; Scheuer, E.; Dibb, J.; Avery, M.; Browell, E.; Sachse, G.; Vay, S.; Blake, D.; Huey, G.; Fuelberg, H. Factors influencing the large-scale distribution of  $Hg^0$  in the Mexico City area and over the North Pacific. *Atmos. Chem. Phys.* **2008**, *8*, 2103–2114.
- (35) Rutter, A. P.; Schauer, J. J. The impact of aerosol composition on the particle to gas partitioning of reactive mercury. *Environ. Sci. Technol.* **2007**, *41* (11), 3934–3939.
- (36) Lynam, M. M.; Keeler, G. J. Artifacts associated with the measurement of particulate mercury in an urban environment: The influence of elevated ozone concentrations. *Atmos. Environ.* **2005**, *39* (17), 3081–3088.
- (37) Talbot, R.; Mao, H.; Feddersen, D.; Smith, M.; Kim, S. Y.; Sive, B.; Haase, K.; Ambrose, J.; Zhou, Y.; Russo, R. Assessment of particulate mercury measured with the manual and automated methods. *Atmosphere* **2010**, *2*, 1–20.
- (38) Landis, M. S.; Stevens, R. K.; Schaedlich, F.; Prestbo, E. M. Development and characterization of an annular denuder methodology for the measurement of divalent inorganic reactive gaseous mercury in ambient air. *Environ. Sci. Technol.* **2002**, *36* (13), 3000–3009.
- (39) Feng, X.; Sommar, J.; Gårdfeldt, K.; Lindqvist, O. Improved determination of gaseous divalent mercury in ambient air using KCl coated denuders. *Fresenius J. Anal. Chem.* **2000**, *366*, 423–428.
- (40) Gustin, M.; Weiss-Penzias, P.; Peterson, C. Investigating sources of gaseous oxidized mercury in dry deposition at three sites across Florida, USA. *Atmos. Chem. Phys.* **2012**, *12*, 9201–9219.
- (41) Ericksen, J. A.; Gustin, M. S.; Schorran, D. E.; Johnson, D. W.; Lindberg, S. E.; Coleman, J. S. Accumulation of atmospheric mercury in forest foliage. *Atmos. Environ.* **2003**, *37* (12), 1613–1622.
- (42) Rea, A. W.; Lindberg, S. E.; Scherbatskoy, T.; Keeler, G. J. Mercury accumulation in foliage over time in two northern mixed-hardwood forests. *Water, Air, Soil, Pollut.* **2002**, *133*, 49–67.
- (43) Huang, J.; Gustin, M. S. Evidence for a free troposphere source of mercury in wet deposition in the Western United States. *Environ. Sci. Technol.* **2012**, *46* (12), 6621–6629.
- (44) USDA Forest service. <http://activefiremaps.fs.fed.us/googleearth.php>.
- (45) Friedli, H. R.; Radke, L. F.; Lu, J. Y.; Banic, C. M.; Leaitch, W. R.; MacPherson, J. I. Mercury emissions from burning of biomass from temperate North American forests: Laboratory and airborne measurements. *Atmos. Environ.* **2003**, *37* (2), 253–267.
- (46) Wang, Y.; Huang, J.; Zananski, T. J.; Hopke, P. K.; Holsen, T. M. Impacts of the Canadian Forest fires on atmospheric mercury and carbonaceous particles in Northern New York. *Environ. Sci. Technol.* **2010**, *44* (22), 8435–8440.
- (47) Holmes, C. D.; Jacob, D. J.; Corbitt, E. S.; Mao, J.; Yang, X.; Talbot, R. W.; Slemr, F. Global atmospheric model for mercury



including oxidation by bromine atoms. *Atmos. Chem. Phys.* **2010**, *10*, 12037–12057.

(48) Weiss-Penzias, P.; Gustin, M.; Lyman, S. N. Observations of speciated atmospheric mercury at three sites in Nevada, USA: Evidence for a free tropospheric source of reactive gaseous mercury. *J. Geo. Res.* **2009**, *49*, 725.

(49) Selin, N. E.; Jacob, D. J.; Yantosca, R. M.; Strode, S.; Jaeglé, L.; Sunderland, E. M. Global 3-D land-ocean-atmosphere model for mercury: present-day vs. pre-industrial cycles and anthropogenic enrichment factors for deposition. *Global Biogeochem. Cycles* **2008**, *22*.

(50) Snider, G.; Raofie, F.; Ariya, P. A. Effects of relative humidity and CO(g) on the O-3 initiated oxidation reaction of Hg-O(g): Kinetic & product studies. *Phys. Chem.-Chem. Phys.* **2008**, *10*, 5616–5623.

(51) Brosset, C.; Iverfeldt, A. Interaction of solid gold surfaces with mercury in ambient air. *Water, Air, Soil Pollut.* **1989**, *43*, 147–168.

(52) Hinds, W. C. *Aerosol Technology: Properties, Behavior, and Measurement of Airborne Particles*; Wiley-Interscience: New York, 1999.

(53) Perraud, V.; Bruns, E. A.; Ezell, M. J.; Johnson, S. N.; Yu, Y.; Alexander, M. L.; Zelenyuk, A.; Imre, D.; Chang, W. L.; Dabdub, D.; Pankow, J. F.; Finlayson-Pitts, B. J. Nonequilibrium atmospheric secondary organic aerosol formation and growth. *Proc. Natl. Acad. Sci.* **2012**, *109* (8), 2836–2841.

(54) Snider, G.; Ariya, P. A. Kinetic and product studies of the reactions of NO<sub>2</sub> with Hg<sup>0</sup> in the gas phase in the presence of titania micro-particle surfaces. *Water, Air, Soil Pollut.* **2012**, *223*, 4397–4406.

(55) Biswas, S.; Verma, V.; Schauer, J.; Cassee, F.; Cho, A.; Sioutas, C. Oxidative potential of semivolatile and non volatile particulate matter (PM) from heavy-duty vehicles retrofitted with emission control technologies. *Environ. Sci. Technol.* **2009**, *43*, 3905–3912.

(56) Pal, B.; Ariya, P. A. Studies of ozone initiated reactions of gaseous mercury: Kinetics, product studies, and atmospheric implications. *Phys. Chem. Chem. Phys.* **2004**, *6* (3), 572–579.

(57) Schroeder, W.; Yarwood, G.; Niki, H. Transformation processes involving mercury species in the atmosphere—Results from a literature survey. *Water, Air, Soil Pollut.* **1991**, *56*, 653–666.

(58) Seigneur, C.; Wrobel, J.; Constantinou, E. A chemical kinetic mechanism for atmospheric inorganic mercury. *Environ. Sci. Technol.* **1994**, *28* (9), 1589–1597.